13

# Portable Optoelectronic Vibration Sensor Based on the Autodyne Effect in a Laser Diode

© A.V. Rybaltovsky, I.S. Mamaev, G.O. Danilenko, V.V. Vitkin, E.E. Popov, A.V. Kovalev

ITMO University,
St. Petersburg, Russia

e-mail: rybaltovskiiav@gmail.com

*Received May 05, 2025*
*Revised September 10, 2025*
*Accepted October 24, 2025*

The operation of a portable remote optoelectronic vibration sensor based on the autodyne effect in a laser diode is demonstrated. The sensor enables the measurement of vibration parameters: frequency (from 10 to 500 Hz) with a relative error of 0.08%, as well as amplitude, velocity, and acceleration with an error of 2.66−2.87%.

**Keywords:** Vibration sensor, Autodyne effect, Laser diode, Remote measurement.

DOI: 10.61011/EOS.2025.11.62916.8097-25

Non-contact monitoring of vibration parameters plays a crucial role in diagnosing the condition of industrial equipment, assessing the structural integrity of buildings and structures, and studying the dynamics of machines and constructions, for example, in robotics and precision systems [1,2]. Traditional contact methods, primarily using accelerometers, impose limitations associated with mounting the sensor directly to the object's surface, which is not always feasible. An alternative to contact methods is provided by non-contact methods, among which optoelectronic methods stand out, enabling high-precision measurements over a wide range of vibration parameters (displacement, acceleration, velocity).

Among optoelectronic technologies, laser Doppler vibrometers (hereafter — LDVs) have gained widespread use. They can provide high measurement reliability, operating in a frequency range up to several megahertz, with picometer-level resolution and at distances up to hundreds of meters from the object [3–5]. Classical LDVs are typically constructed based on Michelson or Mach−Zehnder interferometers using a laser source, multicomponent optical systems for beam formation and recombination, and a photodetector. The drawbacks of LDVs include: structural complexity, high cost, and large size, which limit their use as truly portable or mass-integrable sensors.

A fundamentally different approach, allowing significant simplification of the design and reduction in cost of an optoelectronic vibrometer, involves the use of the autodyne effect in semiconductor laser diodes [2,6,7]. The essence of the effect lies in the interference of radiation reflected or scattered by an external object with the field inside the resonator of the semiconductor laser itself, leading to modulation of the optical power. The photodetector is the photodiode integrated into the laser diode package. This photodiode is a design element of most commercially available laser diodes and serves to monitor the semiconductor laser power. Combining the source and receiver in a single functional unit enables the creation of a compact, energy-efficient vibration sensor with low cost [2]. However, a consequence of this design simplification is more modest performance characteristics compared to LDVs: the frequency range typically does not exceed tens of kilohertz, the resolution is fundamentally limited by half the laser wavelength ($\lambda/2$), and the operating distance is several meters, constrained by the source's coherence length.

Despite the appealing simplicity of the hardware, the primary challenge in developing autodyne vibrometers lies in processing and interpreting the resulting autodyne signal. This signal has a characteristic but often distorted sawtooth shape. Its amplitude, shape, and signal-to-noise ratio strongly depend on the object's reflection coefficient and the atmospheric path transmittance. Existing processing algorithms are often oriented toward extracting only a subset of vibration parameters, require complex computations, or exhibit sensitivity to signal shape variations. This complicates the accurate and, importantly, simultaneous determination of the full set of vibration parameters (frequency, amplitude, velocity, acceleration) under real operating conditions with sufficient reliability for practical applications.

To overcome the aforementioned difficulties related to distortion of the autodyne signal shape and changes in its amplitude, the present work proposes a processing algorithm based on analyzing the temporal positions of the signal extrema (peaks). Unlike methods requiring full waveform analysis, this approach is invariant to slow changes in signal amplitude caused by variations in optical feedback. The key idea is that each sawtooth tooth of the signal, regardless of its amplitude and shape, corresponds to a displacement of the object by half the wavelength of the laser radiation ($\lambda/2$). Thus, by detecting the times of occurrence of these peaks and the moments when the direction of motion changes (inversion of the sign

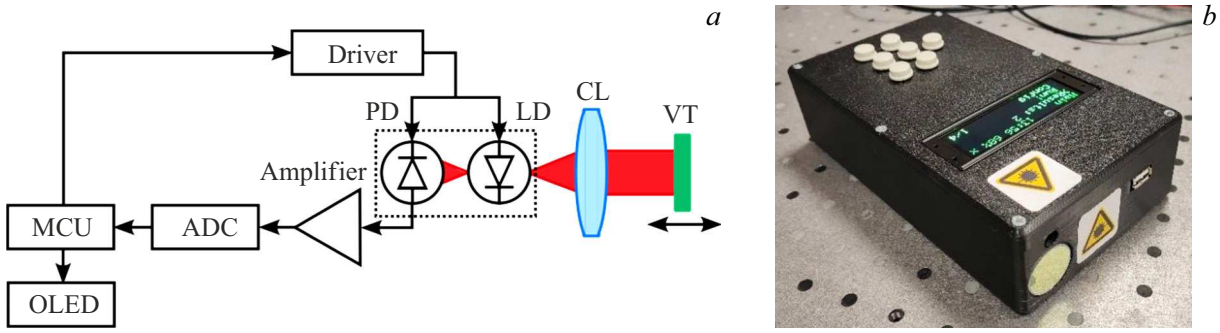


**Figure 1.** Schematic (*a*) and external view (*b*) of the developed vibration sensor in its housing.

of the signal's derivative), all vibration parameters can be reconstructed with high accuracy. This approach is computationally simple, making it ideal for implementation on resource-constrained embedded microcontrollers, and enables the creation of a truly portable and inexpensive device.

The schematic and external view of the portable optoelectronic vibration sensor are shown in Fig. 1. As the radiation source for the developed vibration sensor, a distributed feedback laser diode (hereafter — DFB laser, denoted as LD on the schematic, model LDI-1550-DFB-2.5G) was selected due to its stable single-mode generation and high coherence. In the experiments, the DFB laser operated at a wavelength of 1550 nm with a pump current of 80 mA, providing an output power of 15 mW. This current exceeded the threshold ($\sim 12.5$ A) by more than sixfold, ensuring stable instrument operation far from the low-frequency fluctuation regime. The DFB laser radiation was collimated using an adjustable collimator (CL, model LTN330). The collimated radiation was directed at the vibrating object (VT), reflected from it, and returned to the resonator, where the reflected light interfered with the intracavity field. This interference modulates the DFB laser output optical power, carrying information about the vibration parameters. Changes in optical power are detected by the built-in monitor photodiode (PD).

The photodiode photocurrent passes through a custom transimpedance amplifier (based on the AD8032ARZ chip), after which the voltage signal is digitized by an analog-to-digital converter (ADC, AD9057BRSZ chip) and transmitted to the microcontroller (MCU, STM32F405ZGT6 chip).

The MCU processes the received digital signal to calculate vibration parameters. Additionally, the MCU controls the DFB laser driver (PLD-CW-2000H-ZIF), which sets the DFB laser operating current. The calculated vibration parameters can be displayed on the built-in liquid crystal display (OLED).

Within the theoretical model of the autodyne effect, the laser output power can be expressed as follows [8]:

$$P(\varphi) = P_0(1 + mF(\varphi)), \qquad (1)$$

where $P_0$ — power emitted by the semiconductor laser without optical feedback, $m$ — dimensionless modulation index characterizing the depth of power modulation and depending on the amount of radiation returning to the resonator after reflection from the vibrating object, $F(\varphi)$ — modulation function, $\varphi = 2kS(t)$ — phase shift; $S(t) = s_0 + s(t)$, where $s_0$ —average distance to the measurement object, $s(t)$ is due to vibration.

The analyzed signal exhibits periodic extrema of amplitude every half-period, forming a sawtooth shape over time with pronounced rise and fall fronts. The signal amplitude modulation takes the form of a low-frequency amplitude envelope on a high-frequency sawtooth carrier, stabilized by the constant laser power. The signal shape and amplitude can vary significantly depending on measurement conditions, posing substantial challenges for processing. As the amount of light returning to the laser diode increases, so does the optical feedback, affecting the signal. Examples of such signals are shown in Fig. 2. In Fig. 2, *a*, the sensor is tilted at a larger angle relative to the normal to the vibrating object compared to Fig. 2,*b*.

Each peak in the high-frequency sawtooth structure of the signal arises due to a phase change in the feedback signal by $2\pi$, corresponding to a change in the total optical path „laser–object–laser" by one wavelength ($\lambda$). Consequently, each observed sawtooth peak in the signal indicates displacement of the vibrating object along the sensing axis by a distance strictly equal to half the wavelength of the laser radiation ($\lambda/2$). Moreover, the sign of the slope (first derivative) of the recorded signal directly depends on the instantaneous velocity direction of the object relative to the sensor [8]. Reversal of the object's motion direction leads to inversion of the autodyne signal derivative sign. Since velocity direction reversal in harmonic or quasi-periodic oscillations occurs at points of maximum and minimum displacement, these points mark the boundaries of vibration half-periods and can be identified by the moments of derivative sign change.

This property forms the basis of the algorithm for processing the digitized autodyne signal. To detect and automatically count peaks, the first derivative of the signal is computed. To suppress high-frequency noise that could

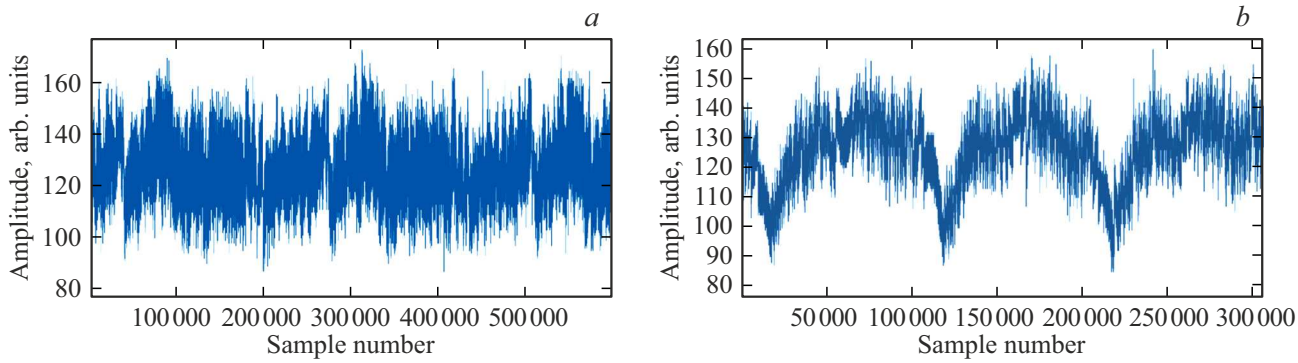


**Figure 2.** Digitized autodyne signals for increasing optical feedback strength from (*a*) to (*b*). The abscissa shows the sample number (sampling frequencies of 4.2 MHz and 2 MHz were used for (*a*) and (*b*), respectively); the ordinate shows signal amplitude in relative units. Distance to object 250 mm, vibration frequency 20 Hz.

cause false triggers during differentiation, the raw signal was pre-smoothed using a moving average with a window size of 7 samples. The first derivative was then computed for the smoothed signal. Sharp intensity changes corresponding to a distance variation of $\lambda/2$ correspond to derivative peaks. These peaks were detected by comparing the absolute derivative value to a threshold set as the mean absolute value of all peaks. For each $n$-th peak, the time coordinate $t_n$ was also determined. Moments of derivative sign inversion correspond to half-periods. Thus, peak detection enables determination of the period and fundamental frequency of vibrations without fast Fourier transform, which is advantageous when the microcontroller has limited computational resources.

The resulting array of peaks and corresponding times is also used to extract vibration parameters from the autodyne signal. The object vibration amplitude is determined as

$$A(t) = kN\frac{\lambda}{2}, \tag{2}$$

where $k$ — calibration coefficient obtained during device calibration, $\lambda$ — laser radiation wavelength, $N$ — number of peaks per half-period, determined as the quotient of the total number of detected peaks $N_p$ divided by the number of detected half-periods $N_{T/2}$:

$$N = N_p/N_{T/2}. \tag{3}$$

Velocity and acceleration are calculated using the formulas:

$$v_n(t) = k\frac{\lambda}{2(t_n - t_{n-1})}, \tag{4}$$

$$a_n(t) = \frac{v_n(t) - v_{n-1}(t)}{t_n - t_{n-1}}, \tag{5}$$

where $v_n(t)$ and $a_n(t)$ — instantaneous object velocity and acceleration calculated for the $n$-th time interval, $v_n(t)$ — instantaneous velocity from the previous step, $t_n$ and $t_{n-1}$ — times corresponding to the $n$-th and$(n-1)$-th detected signal peaks.

As the vibrating object VT in the experimental studies, a low-frequency speaker was used, with its membrane serving as a source of controlled vibrations, to the surface of which aluminum foil was attached. The reflection coefficient of the foil used is approximately 80% at the 1550 nm radiation wavelength. The study was conducted using the developed optical vibration sensor. Measurements were performed non-contact, with an average distance to the vibrating surface of 250 mm.

Harmonic oscillations of the speaker membrane were generated using an AKIP-3420/1 signal generator. A series of measurements was conducted at oscillation frequencies of 10, 50, 100, 200, 300, 400, 500 Hz and amplitudes of 0.83, 0.28, 0.1, 0.045, 0.032, 0.031, 0.0225 mm.

For each frequency-amplitude combination, four independent measurements were performed. The relative error was calculated using the formula:

$$\delta_A = \frac{X_m - X_r}{X_r}, \tag{6}$$

where $X$ — one of the measured parameters (frequency, amplitude, velocity, or acceleration), and $X_m$ and $X_r$ — its measured and true values, respectively.

Analysis of the results (Fig. 3) shows that the errors in determining vibration parameters did not exceed:

— for vibration frequency — 0.08% (Fig. 3, *a*);
— for vibration velocity — 2.87% (Fig. 3,*b*);
— for vibration amplitude — 2.75% (Fig. 3,*c*);
— for vibration acceleration — 2.66% (Fig. 3, *d*).

It is important to note that while frequency measurement accuracy remains consistently high across the entire operating range, errors in other parameters show a clear dependence on their magnitude. This behavior has a physical explanation related to autodyne signal processing features: high errors at small amplitudes and accelerations result from quantization effects and noise amplification during numerical differentiation, while the $U$-shaped dependence for velocity is determined by the balance between low-frequency noise influence and system bandwidth.

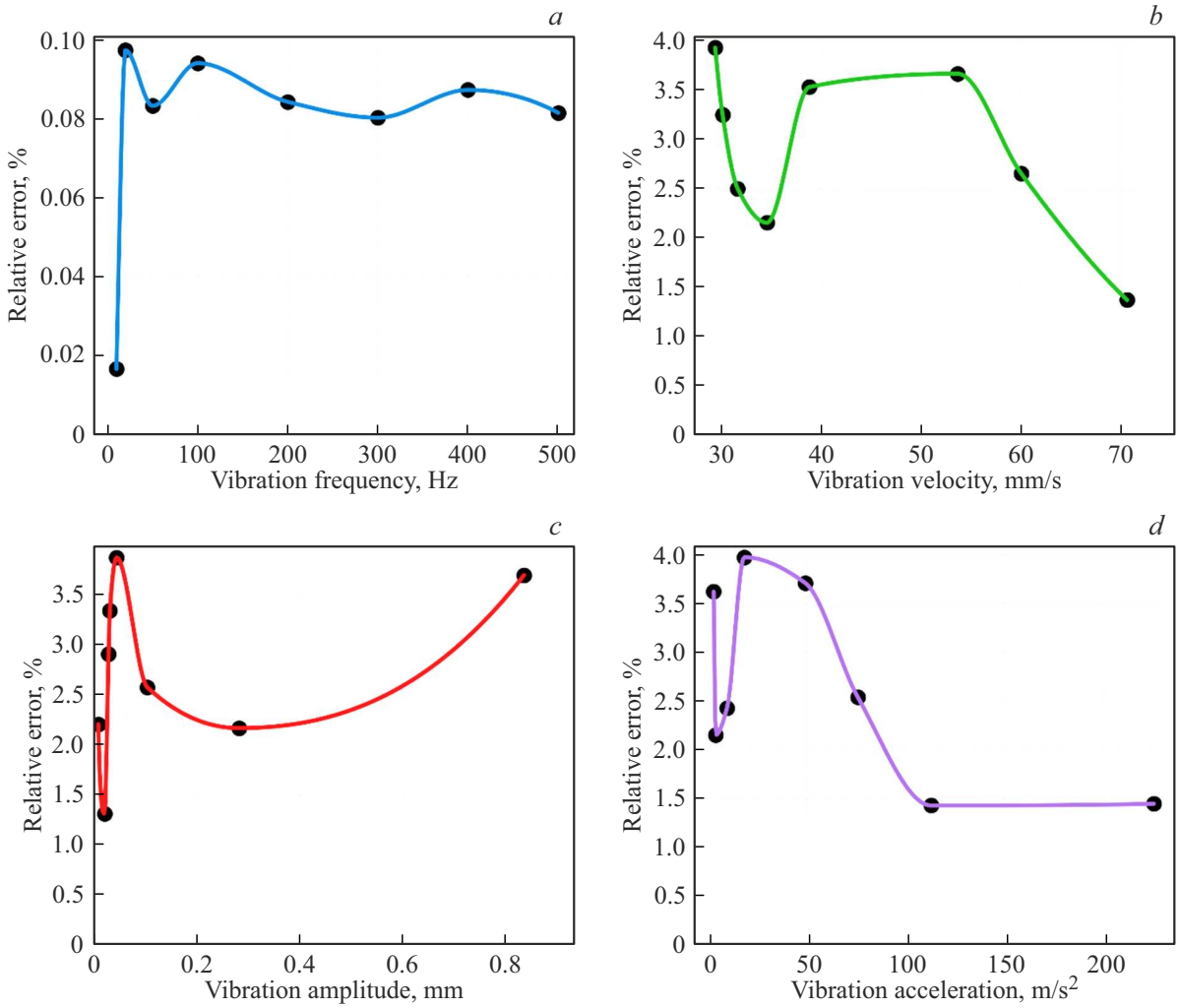


**Figure 3.** Dependence of relative measurement error on the absolute value of the measured vibration parameter for frequency (*a*), velocity (*b*), amplitude (*c*), and acceleration (*d*) of vibrations.

It is known that autodyne signal parameters, including shape and amplitude, depend substantially on distance to the object and feedback coefficient. Under certain conditions, especially weak to moderate feedback, low-frequency intensity fluctuation regimes may arise, which could potentially be mistaken for vibration-related peaks. This effect was not observed in our experiments, achieved thanks to the stability of the vibrating object and, more importantly, operation in the strong optical feedback regime, ensured by appropriate experimental parameters (high target reflection coefficient, operating current sixfold above threshold). However, investigating distance effects on measurement accuracy and developing adaptive algorithms robust to such phenomena is an important task for future work. Additionally, the sensor's maximum operating distance is limited by the laser coherence length. For DFB lasers of this class, the coherence length is typically several meters. Thus, in the experiments at 250 mm to the object, system operation was far from fundamental coherence limitations.

In summary, the paper presents results of experimental validation of a compact remote optoelectronic vibration sensor based on the autodyne effect in a 1550 nm distributed feedback laser. The proposed signal processing method, based on analyzing extrema temporal positions, enables extraction from the digitized autodyne signal of vibration parameters: frequency, amplitude, velocity, and acceleration. The relative frequency measurement error was less than 0.1%, and errors for amplitude, velocity, and acceleration were less than 3%. The results demonstrate the promise of autodyne-based sensors for creating inexpensive, portable, and embeddable solutions for non-contact vibration monitoring.

## Acknowledgments

The authors express special thanks to Evgeny Zinchenko for his contribution to the development and debugging of the sensor's analog-to-digital section.

### Funding

The work on designing the optical and electronic parts of the sensor was supported financially by ITMO University under project № 423020 PO NIOKTR. The work on processing experimental data was supported by the Ministry of Science and Higher Education of the Russian Federation (state assignment № FSER-2025-0025).

### Conflict of interest

The authors declare that they have no conflict of interest.

## References

[1] K. Xu, B. Liu, J. Wang, Y. Wang, Y. Li, Sensors, **23** (22), 9196 (2023). DOI: 10.3390/S23229196
[2] S. Donati, Vib., **6** (3), 625 (2023). DOI: 10.3390/VIBRATION6030039
[3] P. Chiariotti, C. Rembe, P. Castellini, M. Allen, in *Handb. Exp. Struct. Dyn.*, ed. by M. Allen (Springer, New York, 2020), p. 1. DOI: 10.1007/978-1-4939-6503-8_4-1
[4] Y. Zeng, A. Núñez, Z. Li, Mech. Syst. Signal Process., **178**, 109196 (2022). DOI: 10.1016/J.YMSSP.2022.109196
[5] S.J. Rothberg, M.S. Allen, P. Castellini, D. Di Maio, J.J.J. Dirckx, D.J. Ewins, B. Halkon, P. Muno, S. Pai, F. Tomasini, N.A.J. van der Knaap, D. Virden, L. Zizheng, Opt. Lasers Eng., **99**, 11 (2017). DOI: 10.1016/J.OPTLASENG.2016.10.023
[6] G. Giuliani, S. Bozzi-Pietra, S. Donati, Meas. Sci. Technol., **14** (1), 24 (2002). DOI: 10.1088/0957-0233/14/1/304
[7] D. Han, M. Wang, J. Zhou, Opt. Express, **14** (8), 3312 (2006). DOI: 10.1364/OE.14.003312.
[8] L. Scalise, Y. Yu, G. Giuliani, G. Plantier, T. Bosch, IEEE Trans. Instrum. Meas., **53** (1), 223 (2004). DOI: 10.1109/TIM.2003.822194

*Translated by J.Savelyeva*